BIOCHEMISTRY
including biophysical chemistry & molecular biology
Article

Biochemistry **2009,** *48,* 7807–7816 7807
DOI: 10.1021/bi900502g

The Recognition Pathway for the DNA Cytosine Methyltransferase M.HhaI[†,‡]

Hongjun Zhou,[§] Matthew M. Purdy,[§,||] Frederick W. Dahlquist,* and Norbert O. Reich*

Department of Chemistry and Biochemistry, University of California at Santa Barbara, Santa Barbara, California 93106-9510
[§]These authors contributed equally to this study [||]Present address: Affymetrix, Inc., 3450 Central Expressway, Santa Clara, CA 95051

Received March 24, 2009; Revised Manuscript Received June 3, 2009

ABSTRACT: Enzymatic sequence-specific DNA modification involves multiple poorly understood intermediates. DNA methyltransferases like M.HhaI initially bind nonspecific DNA and then selectively bind and modify a unique sequence. High-resolution NMR was used to map conformational changes occurring in M. HhaI upon binding nonspecific DNA, a one base pair altered noncognate DNA sequence, and both hemimethylated and unmethylated cognate DNA sequences. Comparisons with previous NMR studies of the apoenzyme and enzyme−cofactor complex provide snapshots of the pathway to sequence-specific complex formation. Dramatic chemical shift perturbations reaching many distal sites within the protein are detected with cognate DNA, while much smaller changes are observed upon nonspecific and noncognate DNA binding. A cooperative rather than stepwise transition from a nonspecific to a cognate complex is revealed. Furthermore, switching from unmethylated to hemimethylated cognate DNA involves detectable protein conformational changes 20−30 Å away from the methyl group, indicating high protein sensitivity and plasticity to DNA modification.

Bacterial and eukaryotic DNA methyltransferases (MTases)[1] contribute to diverse and essential biological processes (*1*, *2*). MTases carry out key epigenetic reactions in which information transfer between generations occurs in the absence of DNA sequence variations. Because DNA MTases often play critical roles in regulating normal or aberrant gene expression, they are targets for both antibiotic and cancer drug development efforts (*3*−*5*). All DNA MTases use the cofactor *S*-adenosyl-L-methionine (AdoMet) to deliver a methyl moiety either to a cytosine or an adenine and do so in a sequence-specific fashion. Moreover, based on many biophysical and structural studies, all DNA MTases, as well as many other nucleic acid modifying enzymes, stabilize their target base in an extrahelical position, which is essential for catalysis.

A critical aspect of the DNA methyl-transfer reaction is common to all site-specific DNA and RNA modifying enzymes and indeed to enzymes which act on polymeric substrates. Well established early in our understanding is that these enzymes initially bind nonspecifically, followed by a highly efficient search mechanism leading to recognition of the target (cognate) sequence. However, this poses a dilemma for DNA modifying enzymes, requiring the recognition of a particular sequence in the midst of an enormous excess of nonspecific DNA and sites which are closely related by single base pair changes (noncognate sites). Crystallography (*6*−*8*), NMR (*9*−*13*), and biochemical methods (*14*−*18*) have been used to probe the structure and dynamics of protein−nonspecific DNA interactions. Different mechanisms for the nonspecific to specific binding transition have been demonstrated for the few proteins that have structural information available for complexes with both specific and nonspecific DNA along with the free protein. In the case of the HoxD9 homeodomain, several NMR techniques were used to demonstrate that nonspecific and specific DNA share a similar binding mode (*11*). However, significant DNA and protein conformational changes have been observed to accompany the transition from nonspecific to specific binding in several other proteins. Crystal structures of the *Eco*RV endonuclease show that the recognition loop which wraps around the DNA to make base-specific contacts in the cognate complex becomes disordered in both the nonspecific complex and DNA free structure (*8*). Similarly, in NMR studies of the *lac* repressor binding, an unstructured hinge region in the free enzyme remains unstructured upon binding a nonspecific sequence but folds into an α-helix upon binding the specific operator sequence (*9*). *Bam*HI endonuclease structures show two helices that unwind to form many of the base-specific contacts upon binding cognate DNA; these regions remain as helices in the noncognate DNA-bound structure (*6*). Most studies point toward a prominent role for electrostatic interactions between protein side chains and the phosphate backbone in binding nonspecific DNA, though this is apparently not universal (*6*). Also, the importance of water-mediated interactions between the DNA backbone and protein has been noted (*6*, *7*, *9*, *16*, *17*) and suggested to play an important role in allowing the protein to slide along nonspecific DNA in its search for a target site (*7*).

The bacterial cytosine DNA methyltransferase M.HhaI modifies the internal cytosine within its cognate recognition site:

[†]M.M.P. was supported in part by NIH postdoctoral fellowship GM071206.

[‡]Resonance assignments will be deposited in BioMagResBank, www.bmrb.wisc.edu, under BMRB 16395.

*To whom correspondence should be addressed. E-mail: reich@chem.ucsb.edu; dahlquist@chem.ucsb.edu. Phone: (805) 893-8368. Fax: (805) 893-4120.

[1]Abbreviations: MTase, DNA cytosine methyltransferase; AdoMet, *S*-adenosyl-L-methionine; M.HhaI, MTase from *Haemophilus haemolyticus*; NMR, nuclear magnetic resonance; AdoHcy, *S*-adenosyl-L-homocysteine; EDTA, ethylenediaminetetraacetic acid; TROSY, transverse relaxation-optimized spectroscopy; HSQC, heteronuclear single-quantum coherence.

5′-GCGC-3′. Many high-resolution crystal structures of M.HhaI complexed with different DNA molecules are available (*19*−*23*). Reorganization of an essential catalytic loop (residues 80−100) is regulated by sequence-specific protein−DNA interactions that occur ~28 Å away from the catalytic loop. DNA-dependent positioning of the catalytic loop was first observed crystallographically (*19*, *20*); cognate DNA stabilizes the loop-closed conformer while nonspecific DNA leaves the loop in the open conformer (*23*). Correct positioning of this loop is essential for catalysis since Cys81, the active site nucleophile that attacks the target cytosine base at the C-6 position, is ~9.6 Å away in the loop-open conformer. The closed loop conformer is also essential for stabilizing the target cytosine that is flipped out of the DNA duplex and tight DNA binding. Using stopped-flow fluorescence spectroscopy to monitor the environment of Trp residues inserted into the catalytic loop, we observed reorganization of the catalytic loop upon DNA binding in the absence of cofactor using several M.HhaI mutants (*24*). Using this same approach, we recently showed that the opened → closed transition does not occur with noncognate DNA and is controlled by a single hydrogen bond involving Arg240 and the major groove guanosine O-6 moiety (GCGC) (R. A. Estabrook, T. T. Nguyen, N. Fera, and N. O. Reich, submitted). While these studies provide detailed insights into the DNA sequence dependent positioning of the critical loop, they leave unanswered how the protein scaffold responds to the transitions, initiated from the apoenzyme, and moving through the binary complex (enzyme−cofactor), nonspecific DNA complex, and noncognate and cognate complexes. As part of our interest in understanding if and how distal residues contribute structurally and dynamically to the substrate sequence discrimination and catalysis, we have obtained NMR information about each of these intermediates.

MATERIALS AND METHODS

DNA Preparation and Protein Expression. DNA strands Hemi^{top} (5′-CATGGCGCAGTG-3′), Hemi^{bot} (5′-CACTGMGCCATG-3′) and NC^{top} (5′-CATGGCGAAGTG-3′), NC^{bot} (5′-CACTTMGCCATG-3′), where M stands for 5-methyl-2′-deoxycytosine, were obtained from Midland Certified Reagent Co. (Midland, TX) and purified by reverse-phase HPLC as described (*25*). The hemimethylated cognate (Hemi) and noncognate (NC) DNA duplexes (Table 1) were formed by annealing the complementary strands in 10 mM Tris-HCl, 1 mM ETDA, and 50 mM NaCl, pH 8.0, buffer. The resulting duplexes were exchanged into the NMR buffers (described below) using Bio-Gel P2 spin columns (Bio-Rad). The unmethylated cognate and nonspecific DNA duplexes were formed from the self-complementary strands 5′-GATAGCGCTATC-3′ and 5′-GACCAGCTGGTC-3′, respectively, which were obtained from Bioneer (Emoryville, CA) with reverse-phase cartridge purification. The self-complementary duplexes were annealed and buffer exchanged as described above.

The DNA sequences used for this work (Table 1) were chosen balancing previous biochemical studies of similar duplexes with specific requirements for NMR research. The sequences were kept short to minimize the molecular weight. The DNA sequence flanking the M.HhaI GCGC recognition site in the hemimethylated and unmethylated cognate duplexes is necessarily different. Self-complementarity is required to yield a single binding mode for the unmethylated (as well as the nonspecific) duplex, while different flanking sequences are necessary to anneal the hemimethylated (as well as the noncognate) duplex stoichiometrically. Such configurations have been used in previous structural studies on M.HhaI (*21*, *22*). The hemimethylated cognate and noncognate sequences were chosen to match the central portions of oligonucleotide duplexes used in previous binding and kinetic studies with M.HhaI (*25*, *26*). The sequences of the unmethylated cognate and nonspecific duplexes were based on those used in previous crystallographic studies (*21*, *23*).

Table 1: Oligonucleotide Duplexes Used as M.HhaI Ligands in NMR Measurements

duplex name	DNA sequence[a]	K_D[b] (nM)	ref for K_D
hemimethylated cognate	5′-CATG**GCGC**AGTG-3′ 3′-GTAC**CGMG**TCAC-5′	0.02	*25*
unmethylated cognate[d]	5′-GATA**GCGC**TATC-3′ 3′-CTAT**CGCG**ATAG-5	0.2	*25*
noncognate	5′-CATG**GCGA**AGTG-3′ 3′-GTAC**CGMT**TCAC-5′	12−270	*26*
nonspecific[d]	5′-GACCAGCTGGTC-3′ 3′-CTGGTCGACCAG-5′	780[e]	−[c]

[a] "M" represents 5-methyl-2′-deoxycytosine; recognition or noncognate sequence in bold; target base underlined. [b] Estimated K_D in the presence of AdoHcy; data based on measurements for 30−40mer DNA sequences in the same sequence class. [c] R. A. Estabrook, T. T. Nguyen, N. Fera, and N. O. Reich, submitted. [d] Self-complementary. [e] Containing CTT repeats as the central sequence.

The previously described (*27*) His_6-tagged version of the solubility-enhanced Δ324G M.HhaI truncation (*28*) was used throughout this study. Uniformly ^{15}N-labeled M.HhaI was expressed as described (*27*). For sequential backbone assignments of M.HahI in complex with *S*-adenosyl-L-homocysteine (AdoHcy) and hemimethylated cognate DNA, a uniformly ^{2}H-, ^{13}C-, and ^{15}N-labeled sample of M.HhaI was used. This sample was a mixture of protein expressed by the previously described method (*27*) and an updated protocol. This modified protocol involved expressing M.HhaI in *Escherichia coli* ER2566 (New England Biolabs) from the plasmid M.HhaIΔ324-His_6/pET28a (*27*) using the procedures outlined by Gardner and Kay for producing uniformly deuterated proteins (*29*), except that the temperature was lowered to 25 °C just prior to induction with IPTG. In all cases, M.HhaI was purified and quantified as described (*27*).

NMR Spectroscopy. All NMR spectra were recorded at 25 °C on a Varian 600 MHz spectrometer equipped with a four-channel (^{1}H/^{13}C/^{15}N/^{2}H) cold probe and *Z*-axis gradient and analyzed as described previously (*27*). The NMR sample used for backbone resonance assignments contained 440 μM uniformly ^{2}H-, ^{13}C-, and ^{15}N-labeled M.HhaI complexed with the cofactor AdoHcy (obtained from Sigma-Aldrich) and hemimethylated DNA in a 1:4.4:1.9 ratio. Data were collected in a buffer containing 50 mM sodium phosphate, 100 mM NaCl, 1 mM EDTA, 50 mM L-arginine, 50 mM L-glutamic acid, and 0.75% glycerol (pH 6.5) with 5 mM dithiothreitol, 0.02% sodium azide, and 8% (v/v) D_2O added. The sample for the ternary complex with unmethlyated cognate DNA contained 400 μM uniformly ^{2}H-, ^{13}C-, and ^{15}N-labeled protein mixed with AdoHcy and DNA in a ratio of 1:1.5:2.5 in the same buffer as above. For nonspecific and noncognate DNA ternary complexes, uniformly ^{15}N-labeled M.HhaI was premixed with AdoHcy, and DNA was added to a ratio of

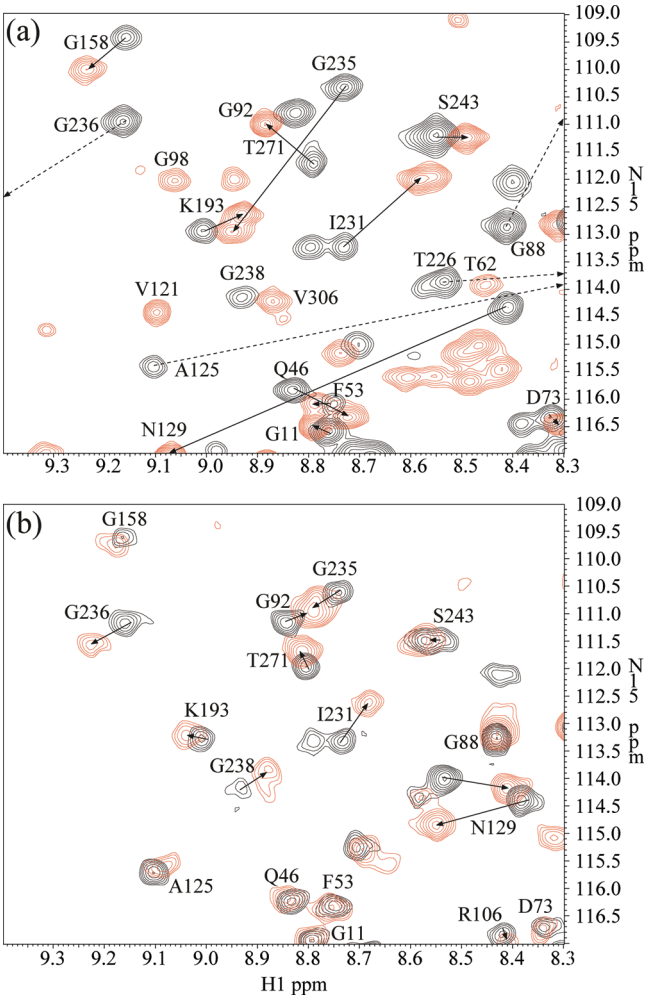

FIGURE 1: Spectral changes of M.HhaI upon binding DNA. A region of the $^{1}H-^{15}N$ correlation spectra is superimposed for the M.HhaI−AdoHcy binary complex alone (black) and the ternary complex (a) bound with hemimethylated cognate DNA (red) or (b) nonspecific DNA (red). In the partially labeled spectra, arrows indicate resonance displacement from the binary to the ternary complex. Dotted arrows denote a few large perturbations (>600 Hz) which have the peaks from the bound states displaced outside the selected region. Note the similarity in the direction of the displacement between the cognate and nonspecific DNA binding for some residues, i.e., N129, I231, and G236.

1:4.5:5.3 and 1:4.0:2.1 with 148 and 115 μM protein, respectively. The samples were in 25 mM sodium phosphate, 50 mM NaCl, and 1 mM EDTA, pH 6.5, buffer with 5 mM dithiothreitol, 0.02% sodium azide, and 8% (v/v) D_2O.

Using the same set of experiments based on the TROSY technique (*30*−*35*) as we performed for the M.HhaI−AdoHcy complex (*27*), we assigned 84% (excluding 12 proline residues and 6 histidines at the C-terminal tag) of the backbone amides in the ternary complex with hemimethylated DNA (Supporting Information Figure 1). This is significantly more than the 76% assigned for the binary complex with AdoHcy. The close similarity of the spectra from the ternary complexes with either hemimethylated or unmethylated DNA allowed us to assign most of the corresponding resonances in the M.HhaI ternary complex bound with unmethylated cognate DNA. Three major segments unassigned in the M.HhaI−cofactor binary complex, residues 107−119, 140−146, and 160−170, remained unassigned in the ternary complex although the unassigned segments were shortened. There are too few cross-peaks remaining in the

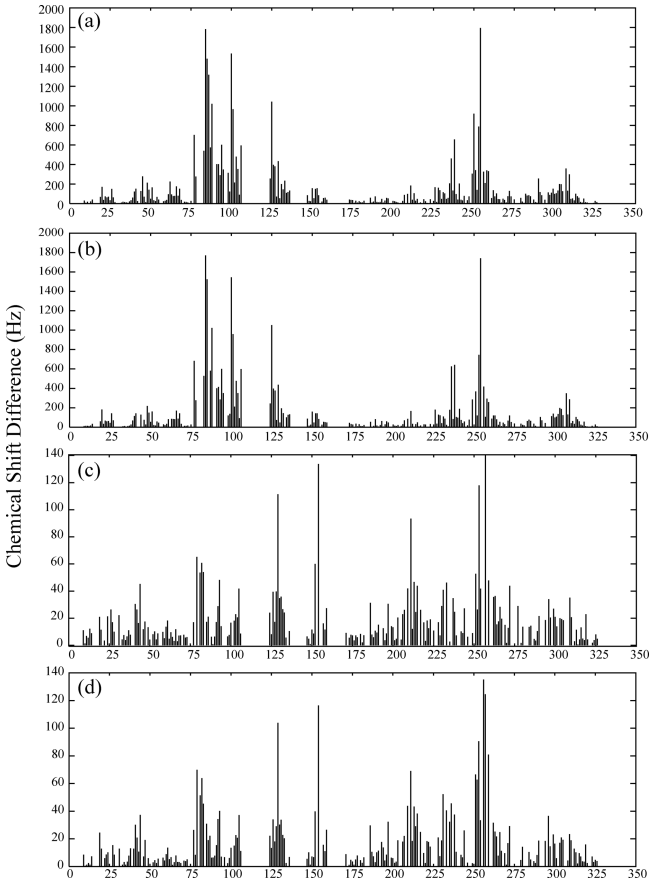

FIGURE 2: Chemical shift perturbations and differences of M.HhaI with DNA. The chemical shift changes (in Hz) between the M.HhaI−AdoHcy binary complex and the ternary complex bound with hemimethylated cognate DNA (a), unmethylated cognate DNA (b), noncognate DNA (c), and nonspecific DNA (d) are plotted as a function of residue number. The shift differences were calculated as the combined differences for the amide ^{1}H and ^{15}N nuclei, equivalent to the displacement magnitudes of the amide peaks as measured at the ^{1}H field of 600 MHz.

$^{1}H-^{15}N$ correlation spectrum to account for all the unassigned residues.

Chemical shift perturbation experiments for interactions with nonspecific and noncognate DNA were done with ^{15}N-labeled M.HhaI samples. Nearly all of the amide resonances assigned for a perdeuterated $^{15}N/^{13}C$-labeled M.HhaI−AdoHcy binary complex could be transferred to a ^{15}N-labeled, fully protonated binary complex. Assignments of the resonances from M.HhaI bound with nonspecific DNA were made with a titration experiment. Most of the resonances could be assigned by superimposing the spectra from the ternary and binary complexes. Some were assigned by tracking the movements of the resonances during the titration. Due to the line broadening that occurred as DNA was added, some assignments could not be reliably transferred and were not used in further analysis. Line broadening is particularly severe in the early titration points of M.HhaI with noncognate DNA. Nevertheless, a great majority of the resonances from M.HhaI bound with nonspecific DNA and noncognate DNA were nearly identical, allowing transfer of assignments based on those made for M.HhaI bound with nonspecific DNA.

RESULTS

Cognate DNA Causes Drastic Chemical Shift Changes in M.HhaI. To assign the spectrum of M.HhaI bound with the

cofactor AdoHcy and cognate DNA (recognition sequence GCGC, where the central cytosine is the methylation site), we chose to use hemimethylated cognate DNA (Table 1) because M.HhaI gave slightly sharper resonances and more uniform peak intensities when bound with this DNA than with unmethylated cognate DNA. Compared with the cofactor bound binary complex, more resonances are observable in this 45 kDa ternary complex. We attributed the missing resonances in the binary complex mostly to exchange dynamics leading to line broadening (*27*); it appears that such dynamics are reduced upon cognate DNA binding but are not entirely removed.

Binding of either unmethylated or hemimethylated cognate DNA to the cofactor-bound binary complex led to dramatic changes in the $^{1}H-^{15}N$ correlation spectrum (Figures 1 and 2). Plotting these changes onto the M.HhaI structure highlights the area of M.HhaI contacting the DNA (Figure 3), as a majority of these large perturbations take place proximal to the DNA duplex. The biggest changes are seen in the catalytic loop (residues 80−99) which moves up to 25 Å when comparing the crystal structure of the M.HhaI−cofactor binary complex with those of M.HhaI−cofactor−cognate DNA ternary complexes and in the DNA recognition loops (residues 234−240 and 249−258) which make base-specific contacts in the major groove (*20*). The combined ^{1}H and ^{15}N perturbations reach up to 1800 Hz with a median peak displacement of 62 Hz. It appears that the entire region from Ala77 to Leu136, incorporating a strand−loop−strand−loop−helix structure, is significantly perturbed with many residues exhibiting shift changes over 400 Hz, although residues 107−119 have not been assigned. One cluster of residues in this highly perturbed region, including Phe124, His127, and Thr132, makes more extensive contacts with the catalytic loop in its closed conformation than in its open conformation. Through site-directed mutagenesis and crystallography, these residues were previously shown to be critical in modulating M.HhaI's ability to discriminate between cognate and noncognate substrates by maintaining the stability of the closed catalytic loop conformation (*36*). Changes in secondary structure in the loop region upon closure are reflected in the Cα chemical shift changes (*37*, *38*). Positive Cα shift changes of 1−3 ppm are observed for residues 79−86, reflecting a change from extended structure in the binary complex to a loose helical structure in the ternary complex. Residues 93−97 form a short helix in the binary complex, but this region is pulled to an extended structure to accommodate the insertion of the loop tip into DNA. This structural change results in a negative 2−3 ppm change in Cα chemical shifts.

Perturbations to remote sites are clearly visible upon DNA binding to the enzyme−cofactor binary complex (Figure 3). This is similar to the protein's response to cofactor binding to the free enzyme (*27*) but with different residues perturbed in this case. Examples of such distal sites include Asn189 and Asp174, approximately 26 and 36 Å away from the DNA duplex, with changes of 73 and 37 Hz, respectively. Glu66 and Thr68 are perturbed with 176 and 151 Hz shift changes but are 22 and 25 Å away from the DNA, respectively. These four residues are found on the protein surface and are also distant from the catalytic loop in crystal structures of both its open and closed forms, suggesting that these changes are not a direct result of interaction with either the DNA or catalytic loop. The presence of these distal perturbations indicates that structural rearrangement has occurred way beyond the immediate DNA binding area. Whether these distal changes result from secondary structural adjustments at the local level or concerted, global structural changes remains unclear.

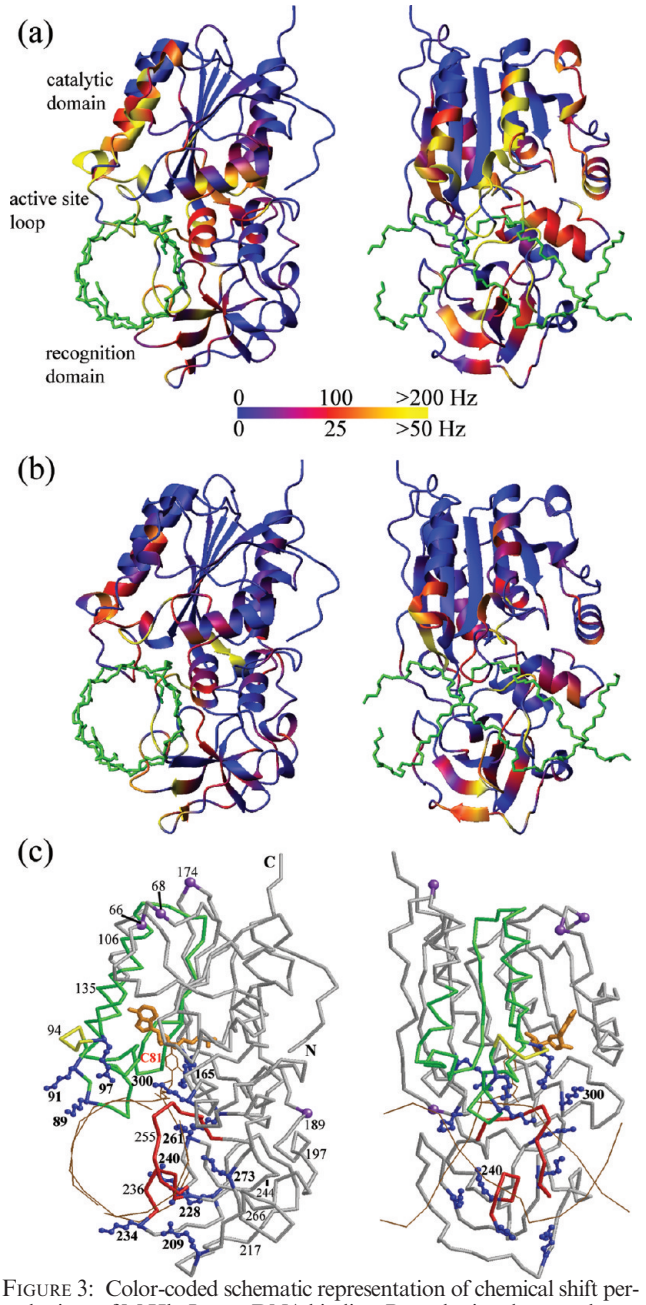

FIGURE 3: Color-coded schematic representation of chemical shift perturbations of M.HhaI upon DNA binding. Perturbation data are shown for binding of the cofactor-bound binary complex with hemimethylated cognate DNA (a) or nonspecific DNA (b). In the left panels, the M.HhaI−cofactor−DNA ternary complex (PDB ID 2HR1 (*52*)) is oriented so that the bound DNA (in green) is viewed down its helical axis. The right panels result from a 90° rotation of the structures in the left panels around the vertical axis. The chemical shift changes are coded in a linear fashion into a color scheme ranging from dark blue to yellow, representing perturbations ranging from 0 Hz (blue) to >200 Hz (yellow) in (a) and from 0 Hz to >50 Hz in (b). The perturbations larger than the higher threshold of 200 or 50 Hz are displayed as yellow, and unassigned residues are also displayed as blue. In (c), a backbone Cα trace is drawn with some residues highlighted and labeled. Two regions with extensive chemical shift perturbations upon binding cognate DNA are colored, with the recognition loops (residues 234−240 and 249−258) in red and a region (residues 77−136) encompassing the active site loop in green. The cofactor, not shown in the top two panels for better clarity of the figures, is shown in gold near the middle of the figures in (c). The active site residue C81 is labeled in red. The arginine and lysine residues that form a strong positively charged surface near the DNA binding site are labeled with bold letters with side chains shown in blue. Residues 93−97 switch to a more extended structure in the ternary complex and are colored in yellow. Four residues distal from the active site having chemical shift perturbations larger than 35 Hz upon binding hemimethylated cognate DNA are shown with purple balls at the Cα positions.

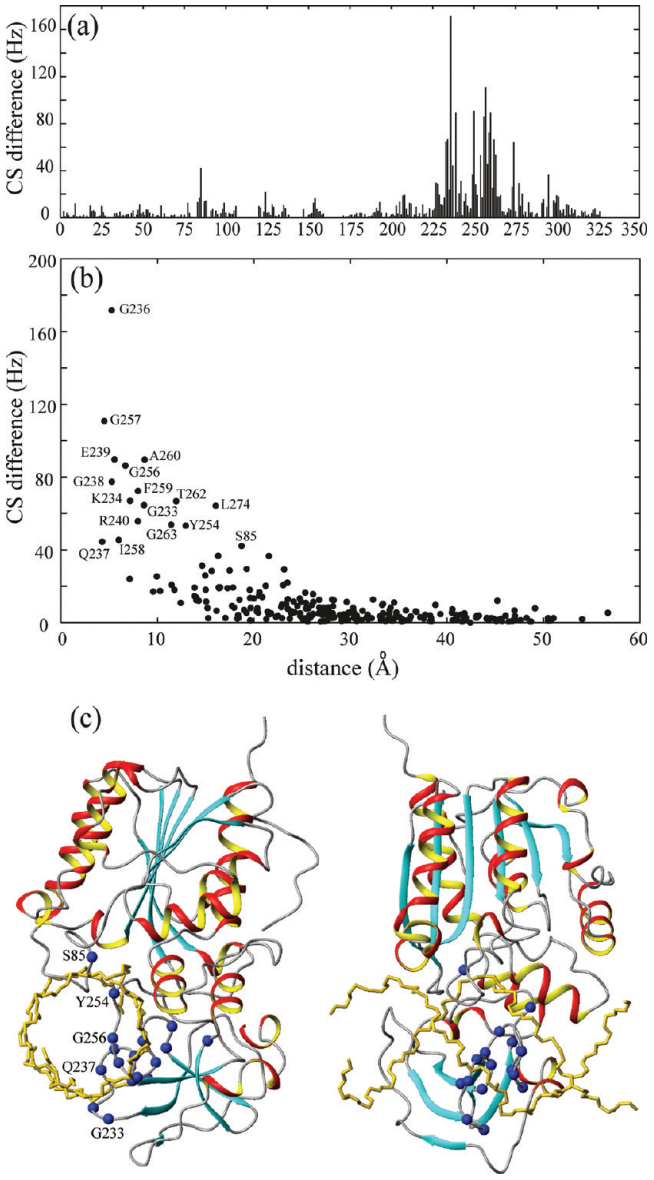

FIGURE 4: Chemical shift differences between M.HhaI binding to unmethylated and hemimethylated cognate DNA. (a) The chemical shift (CS) differences are calculated between the assigned resonances in the $^{1}H-^{15}N$ correlation spectra from M.HhaI bound with either unmethylated cognate or hemimethylated cognate DNA. (b) The chemical shift difference is plotted as a function of the distance measured from the C-5 methyl carbon of the central cytosine to the backbone amide nitrogen. The distance is based on the crystal structure of M.HhaI bound with the cofactor AdoHcy and a hemimethylated cognate DNA (PDB ID 5MHT (*22*)). Residues with shift differences larger than 40 Hz are labeled. (c) The residues that show chemical shift differences larger than 40 Hz are depicted as blue dots at the backbone Cα positions. Only a few residues are labeled for clarity. The right figure results from a 90° rotation of the left figure around the vertical axis.

Comparison of Hemimethylated and Unmethylated Cognate DNA Binding. We observe sharper resonances and more uniform intensities in M.HhaI spectra with hemimethylated cognate DNA in comparison to unmethylated cognate DNA. Hemimethylated DNA is bound more tightly than unmethylated DNA (*25*), which we speculate results in less conformational exchange and intermolecular association between different M.HhaI−DNA complexes than with unmethylated DNA. Alternatively, alteration of the DNA sequence flanking the GCGC recognition site to accommodate the formation of a hemimethylated duplex (see Materials and Methods) may have allowed a more unique binding mode to be established in the ternary complex. Both properties favor better NMR quality.

Comparing hemimethylated and unmethylated cognate DNA binding, we observe similar patterns and magnitudes of perturbations, and the maximum difference (~170 Hz) is substantially smaller than the perturbation seen for either DNA binding to the enzyme−cofactor complex (Figure 4 and Supporting Information Figure 2). A majority of the differences between these two cognate complexes are within the line widths of the resonances. Plotting the largest differences (>40 Hz) onto the M.HhaI structure shows that almost all of the significantly affected residues are located in or near the two DNA binding loops, residues 234−240 and 249−258, in the recognition domain (Figure 4c). Among them Arg240 contacts the O-6 of the guanine 5′ to the flipped cytosine, and this interaction is critical for the stabilization of the catalytic loop in the closed conformation (R. A. Estabrook, T. T. Nguyen, N. Fera, and N. O. Reich, submitted). Glu239 is in close contact with the cytosine C-5 methyl group of the nontarget DNA strand and was suggested to confer M.HhaI's preference for binding hemimethylated over unmethylated DNA (*22*, *25*, *39*, *40*). Moreover, these differences radiate far from the methylation site and are visible from a 20−30 Å distance (Figure 4b).

We observe a clear correlation between a residue's distance from the cytosine C-5 methyl carbon and its chemical shift difference between the hemimethylated and unmethylated DNA complexes (Figure 4b). This indicates that most of the peak perturbations are caused directly by the single methyl group change. The perturbation differences between hemimethylated and unmethylated DNA cluster around the central GCGC target region, suggesting that the observed differences are truly due to the presence of the methyl group and not the changes in the flanking DNA sequence. The active site loop region exhibits small, mostly <20 Hz differences, indicating the structure of this area in the two DNA-bound states is essentially the same. This is consistent with the small difference in methylation rates between hemimethylated and unmethylated cognate DNA (*25*). In summary, the recognition domain clearly is able to distinguish the difference of a single methyl group in the DNA and is mainly responsible for M.HhaI's preference for binding hemimethylated DNA (*22*, *25*).

Binding to Nonspecific and Noncognate DNA. Instead of the cognate sequence GCGC, the nonspecific DNA chosen for this work contains the central sequence CAGCTG while the noncognate DNA contains GCGA, one base modified from the cognate sequence (Table 1). In contrast to the large perturbations seen with either hemimethylated or unmethylated cognate DNA, the response of M.HhaI to nonspecific and noncognate DNA is more muted (Figures 1b and 2c,d). Chemical shift perturbations with the cofactor or nonspecific DNA are down by a factor of 10 or more from those seen with cognate DNA for 33% of the residues. The overall patterns of the perturbations, but not the magnitudes across the sequence, are somewhat similar to those observed for cognate DNA binding (Figures 1 and 2). However, the perturbations upon binding nonspecific and noncognate DNA are more focused around the DNA binding site and skew more toward the recognition domain (residues 191−275), especially residues 209−215 near the surface (Figures 2 and 3). In addition, a few residues more than 12 Å away from the DNA binding site are among the 25% of residues most impacted by nonspecific DNA binding. These include Leu197 and Thr244 and Leu266 on or near the

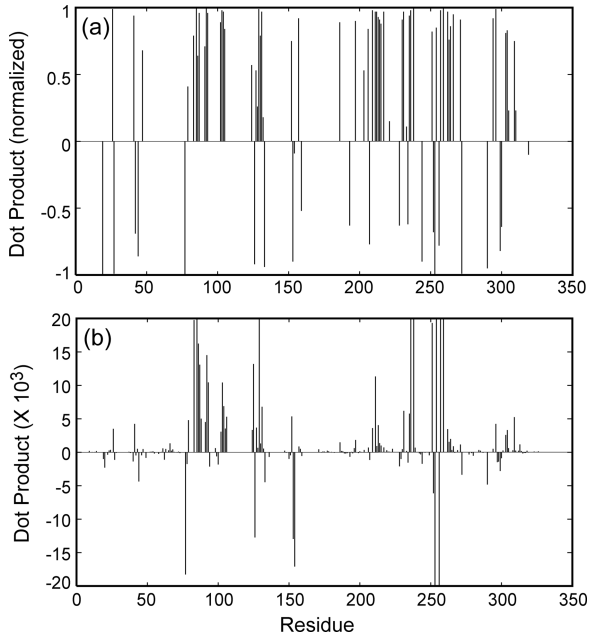

FIGURE 5: Directional similarity between amide chemical shift perturbations with nonspecific and hemimethylated cognate DNA. The similarities of chemical shift perturbations upon binding these two types of DNA are examined in terms of the direction and magnitude of the resonance movement from the binary state to the ternary state. A displacement vector is defined as the vector starting from a peak in the $^{1}H-^{15}N$ correlation spectrum from the binary complex and ending at the shifted peak after the addition of DNA. For each residue two displacement vectors are extracted from binding to cognate and nonspecific DNA, and their mathematical dot product is calculated. The dot product between two vectors **A** and **B** is $a \cdot b \cdot \cos(\theta)$, where a and b are the length of the vectors forming an angle θ. (a) The normalized dot product or $\cos(\theta)$ of the two amide displacement vectors with the two types of DNA for each residue ranges from +1 (parallel displacements) to −1 (antiparallel displacements); zero indicates the two displacements are perpendicular to each other. Residues with perturbations less than 15 Hz are excluded from the figure to account for uncertainty in peak position measurement. (b) The unnormalized dot product ($a \cdot b \cdot \cos(\theta)$) is effectively weighted by the magnitudes of the displacements, thus revealing similarity in both direction and magnitude of the two displacements.

surface of the small domain, Phe186 in the connector between the two domains, Asn309 near the surface of the large domain, and Asp105 near the catalytic loop in its open form.

The residue-specific perturbations for the nonspecific and noncognate DNA very much resemble each other. The small spectral differences seen between binding these two types of DNA are almost entirely located in the recognition domain, primarily involving residues in the two DNA-binding loops, Leu251−Gly263 and Gly233−Arg240 (Figure 2c,d and Supporting Information Figure 3). Binding noncognate and nonspecific DNA also causes significant line broadening to all residues when the ratio of DNA to protein concentration is less than 1, suggesting multiple M.HhaI molecules may likely bind to one DNA molecule when the DNA concentration is low as previously indicated by electrophoretic mobility shift assays (*23*). This process increases the average molecular size and chemical exchange, leading to line broadening in the $^{1}H-^{15}N$ correlation spectrum. We observe that resonances move toward the bound positions before broadening takes place and sharpen as more DNA is added to exceed 1 equiv of protein. Line broadening is more severe with noncognate DNA under the same condition as for nonspecific DNA binding, in line with M.HhaI's higher affinity for noncognate sequences than nonspecific sequences (*26*) (R. A. Estabrook, T. T. Nguyen, N. Fera, and N. O. Reich, submitted).

Differences and Similarities between Nonspecific and Cognate DNA Binding. The rarely observed, dramatic chemical shift perturbations with cognate DNA are consistent with the 25 Å movement of the active site loop and insertion of the recognition loops deep into the DNA major groove. The 10-fold reduction in shift perturbation with nonspecific and noncognate DNA indicates no such coordinated structural changes occur and the active site loop remains essentially in an open state. However, the residual similarity observed between the chemical shift perturbation patterns caused by cognate and nonspecific DNA binding prompted us to ask whether the presence of fast to intermediate time scale exchange observed in nonspecific DNA binding would involve a component resembling the bound state with cognate DNA. Although we do not expect the patterns of perturbations to be the same for different types of substrates even with the same underlining kinetics, we speculate that those residual perturbations due to mostly structural changes resembling active site loop closure and recognition loop contact seen with cognate DNA may be present in binding to nonspecific and noncognate DNA sequences. Even with a small population, the presence of this specific, bound state with its large chemical shift changes could be reflected in the correlation of the magnitude and/or direction of resonance displacements in the cognate and nonspecific DNA binding.

We analyzed this correlation by calculating the dot products between the amide resonance displacement vectors from its position in the binary complex in the $^{1}H-^{15}N$ correlation spectra with the addition of either cognate or nonspecific DNA (Figure 5). The normalized dot product is simply the cosine of the angle between the two displacement vectors and is a direct measure of the directional similarity. We found that roughly 70% of the resonances are perturbed with cognate and nonspecific DNA in almost the same direction away from the binary complex, with the normalized displacement vector dot product close to +1. The unnormalized dot products of the vectors reflect the overall similarity in both the direction and magnitude of the displacements. This analysis shows that the overall perturbations, particularly those associated with the biggest shift changes, are similar in the displacement direction and somewhat correlated in magnitude of movement. These correlations suggest that M.HhaI interactions with nonspecific and noncognate DNA mimic those with cognate DNA to some extent, suggesting the bound state specific to the cognate DNA is being sampled by nonspecific DNA. It is also possible, although less likely, that the residual similarity we observed is a coincidental effect of multiple independent, mostly nonspecific binding events. Overall, the much weaker affinity of M.HhaI for the nonspecific and noncognate DNA and the much smaller, overall disproportional perturbations indicate that the nonspecific DNA do not have a unique binding mode and lack the characteristics that allow a cooperative, simultaneous closure of the active site loop and close contacts with the recognition loops. Thus, these complexes may sample among a variety of sites and orientations, including the specific conformation, and the active site loop is mostly in the open state as observed for the binary complex.

DISCUSSION

Drastic Differences between Cognate and Nonspecific DNA Binding. Our NMR data of M.HhaI in complex with

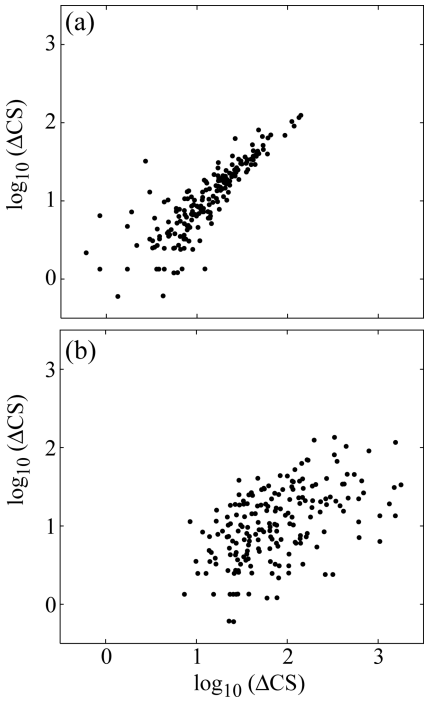

FIGURE 6: Correlations between chemical shift perturbations of M. HhaI upon binding to different DNA sequences. Each dot represents combined chemical shift perturbations (ΔCS, in Hz) for one amide due to binding to (a) noncognate and nonspecific DNA or (b) hemimethylated cognate DNA and nonspecific DNA. The data from nonspecific DNA are plotted along the *Y*-axis. The larger data scattering for smaller perturbations is most likely due to the larger relative uncertainties contained in small perturbations measured.

various DNA molecules agrees with and extends prior crystallographic studies by providing information about additional complexes. Comparison of the M.HhaI−cofactor binary complex crystal structure with that of M.HhaI−cofactor−DNA ternary complexes shows a large conformational change of the catalytic loop (residues 80−99) with some residues moving up to 25 Å (*19*, *20*). Upon binding cognate DNA, the largest chemical shift changes (reaching up to almost 2000 Hz) were found in the catalytic loop and in recognition domain residues that contact the DNA. In contrast, little difference in the loop conformation was observed in comparing structures of the M.HhaI−cofactor binary complex with that of the same complex crystallized in the presence of nonspecific DNA (*19*, *23*). Though no DNA appeared in the crystal, a templating effect of the nonspecific DNA was inferred from the observed cofactor reorientation in its binding site. Here, using the same nonspecific DNA sequence (except one base pair shorter), we directly observed its effect through chemical shift perturbations on M.HhaI in solution state. Our data show that M.HhaI binds to the nonspecific DNA with a low micromolar affinity, consistent with that previously observed (*23*) (R. A. Estabrook, T. T. Nguyen, N. Fera, and N. O. Reich, submitted). The patterns of chemical shift perturbations share some similarities with cognate DNA binding, but the magnitudes are on the order of 10 times smaller for the most perturbed residues. The data indicate that the binding mode is likely very different between nonspecific and specific DNA.

Drastic Binding Change from One-Base Modification. In addition to comparing chemical shift perturbations with cognate (recognition sequence GCGC) and nonspecific DNA complexes (containing the central sequence CAGCTG), we have also collected binding data for a one base modified sequence deemed a noncognate sequence (containing GCGA). The progression from cognate to noncognate to nonspecific then removes one base pair from the recognition sequence at each step of the way. Our data show that the noncognate DNA complex has chemical shifts very similar to those of the nonspecific complex rather than a state halfway between cognate and nonspecific. Further evidence for this is shown in Figure 6 where the chemical shift perturbations for each residue are plotted for the two types of DNA. A nearly linear correlation is observed between perturbations by nonspecific and noncogate DNA. In contrast, only a weak correlation is seen between the perturbations by cognate and nonspecific DNA binding. Plotting these data separately for the small and large domains does not lead to obvious improvement in the correlation curves. A similar conclusion was derived from fluorescence measurements with a tryptophan reporter incorporated into the catalytic loop (*24*) (R. A. Estabrook, T. T. Nguyen, N. Fera, and N. O. Reich, submitted). Here the loop conformation of M.HhaI with either nonspecific or noncognate DNA molecules resembled that of the M.HhaI−cofactor binary complex, while a large change in loop reporter fluorescence accompanied cognate DNA binding. This also mimics the trend measured for DNA binding affinities where M.HhaI had an affinity for a one base altered noncognate DNA sequence only slightly better than that for a nonspecific sequence (R. A. Estabrook, T. T. Nguyen, N. Fera, and N. O. Reich, submitted). These data indicate that the interaction of M.HhaI with cognate DNA is highly selective and cooperative, and similar nonspecific interactions are responsible for binding with both nonspecific and noncognate DNA.

Electrostatics are known to make a significant contribution toward nonspecific binding, and the surfaces of nucleic acid binding proteins are highly enriched in positive charges from arginine and lysine side chains. Indeed, in many cases a simple electrostatic potential map reveals the nucleic acid binding site (*41*, *42*). Electrostatic forces can enhance the diffusion-controlled association rate (*43*, *44*) through "electrostatic steering" (*45*, *46*). Electrostatic interactions appear to be largely responsible for the nonspecific binding of the *lac* repressor (*9*). For M.HhaI, we observed a strong salt effect on the strength of nonspecific and noncognate DNA binding. With the addition of 200 mM NaCl, M.HhaI binding to nonspecific DNA was almost weakened to beyond detection in our titration experiment at the >100 μM protein and DNA concentrations reported here. Further examination of the M.HhaI structure and construction of an electrostatic potential map (results not shown) revealed a unique clustering of positive charges near the cognate DNA binding site contributed by Lys162, Arg165, Arg209, Arg228, Lys234, Arg240, Lys261, Lys273, and Lys300 from the recognition domain and Lys89, Lys91, and Arg97 from the active site loop (Figure 3c). The skewing of these charges toward the recognition domain side of M.HhaI's DNA binding site, combined with a major contribution of electrostatics to nonspecific DNA binding, may help to explain why the largest chemical shift perturbations upon binding nonspecific DNA are distributed more into the small domain than was observed upon binding cognate DNA (Figures 2 and 3).

Together, these data cover a broad range of possible interactions involving M.HhaI in solution and confirm that the transition from nonspecific to specific DNA binding requires a large protein conformational change involving simultaneous, cooperative interactions with the active site loop and recognition domain; importantly, this conformational change does not predominate if

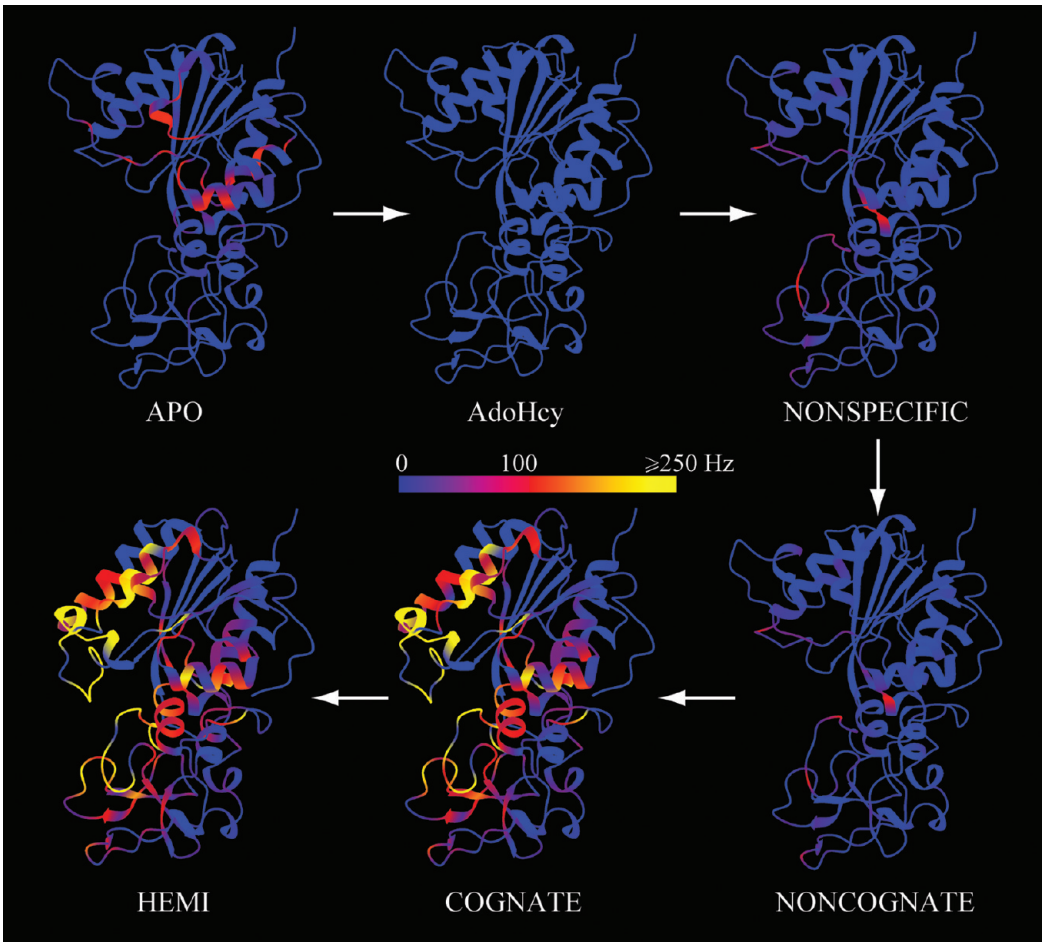

FIGURE 7: M.HhaI chemical shift perturbations by cofactor and DNA. Relatively small shift changes were seen with the cofactor (maximum ~150 Hz) and nonspecific and noncognate DNA (maximum ~150 Hz). As the central base sequence changes incrementally toward the cognate sequence (methylated or unmethylated), sudden and drastic perturbations up to 2000 Hz were observed. All perturbations were relative to the cofactor-bound binary complex and measured as the combined ^{1}H and ^{15}N resonance displacement (in Hz) at the ^{1}H frequency of 600 MHz. Chemical shift perturbations were coded linearly into a color scheme where blue corresponds to no perturbation (or an unassigned residue) and yellow corresponds to the largest perturbation (> 250 Hz). The color mapping is done for shift perturbations within the range of 0−250 Hz. Residues showing combined shifts larger than 250 Hz appear in yellow.

even a single base pair is altered within the recognition sequence. This stands in contrast to previous findings where residual dipolar coupling and paramagnetic relaxation studies implicated that the HoxD9 homeodomain uses the same protein interface to bind both specific and nonspecific DNA (*11*). M.HhaI's transition from nonspecific to cognate DNA binding may more resemble that seen in NMR studies of *lac* repressor binding where rearrangement of a helical protein segment and a tilt in the DNA with respect to the protein interface were observed when comparing specific to nonspecific DNA binding (*9*). Further dynamical, residual dipolar coupling, and paramagnetic relaxation measurements are needed to identify the binding mode of nonspecific and noncognate DNA to M.HhaI.

Implications for Cytosine Base Flipping. Comparison of the affinities of M.HhaI for various DNA sequences shows about a 1000-fold increase in apparent equilibrium binding affinity for cognate sites as compared to noncognate sites (*26*) (R. A. Estabrook, T. T. Nguyen, N. Fera, and N. O. Reich, submitted). Nonspecific site complexes with M.HhaI are at least 4-fold weaker than noncognate sites and about 4000-fold weaker than cognate sites (R. A. Estabrook, T. T. Nguyen, N. Fera, and N. O. Reich, submitted). These approximations are based on a comparison to the unmethylated cognate substrate (Table 1). However, the similarity in the chemical shifts we observe for M.HhaI with the noncognate and nonspecific DNA suggests that they share a similar structure where the bulk of the DNA has the target cytosine base in a normal Watson−Crick base-paired configuration and the loop repositioning that accompanies and stabilizes the flipped out cytosine is not favored. This conclusion is supported by recent observations using a fluorescent reporter sensitive to motion of loop residues when the flipped out base is stabilized (R. A. Estabrook, T. T. Nguyen, N. Fera, and N. O. Reich, submitted).

Spontaneous base flipping is a relatively rare event, being some 10−20 kcal/mol less stable than the normal DNA duplex configuration (*47*−*49*). However, M.HhaI will methylate noncognate sequences with rates for the methylation step (k_{chem}) only 10−~500-fold lower than the values for the cognate sequence depending on which noncognate sequence is under investigation (*26*). This strongly supports the notion that the enzyme can flip out the cytosine base in noncognate sequences as well as cognate sequences. However, it appears that the enzyme cannot stabilize the flipped out configuration sufficiently to make it the predominant form in noncognate DNA complexes at equilibrium. Comparison of the rate constants for methylation of cognate and noncognate sites suggests that between 0.2% and 10% of M.HhaI noncognate DNA complexes (depending on the sequence) may exist in the flipped out configuration assuming

that the rate constant for methylation is the same for cognate and noncognate sequences once in the flipped out configuration.

How Does M.HhaI Find Its Target Site? A summary of the chemical shift changes we have observed in different complexes is shown in Figure 7 where the observed combined shifts are color-coded on the M.HhaI−AdoHcy binary or M.HhaI−AdoHcy−cognate DNA ternary complex crystal structures. These chemical shift changes suggest a "pathway" from the apo state to the ternary complex of M.HhaI, AdoHcy, and hemimethylated DNA. This "pathway" is a reasonable representation of the energy landscape M.HhaI experiences as various ligands bind but may not represent the true kinetic path between the free and bound states.

Our NMR data, along with fluorescence (*24*) (R. A. Estabrook, T. T. Nguyen, N. Fera, and N. O. Reich, submitted) and crystallographic data (*19*, *20*, *23*), support a mechanism for site-specific DNA recognition where the enzyme searches along DNA for its GCGC recognition site predominantly in a loop open position, only closing the loop around the active site either very rarely during the search process or only once the target sequence is found. In related systems, endonuclease pausing at sites resembling their recognition sequence has been proposed (*50*, *51*). In the case of M.HhaI, the similarity of the loop conformation in binding nonspecific and noncognate sequences by both the previous loop reporter fluorescence (*24*) (R. A. Estabrook, T. T. Nguyen, N. Fera, and N. O. Reich, submitted) and current NMR data suggests that as the enzyme searches DNA for its cognate site, it may not dwell on noncognate sites, where one of the four bases is altered from its target sequence, preferentially over nonspecific sites.

The NMR data appear to be consistent with the view that M. HhaI could scan the DNA sequence for suitable methylation sites by binding and potentially flipping out bases in nontarget sequences and then using the complementarity of interactions between the DNA bases and the protein to establish the correct site for methylation. We do not observe a great deal of selective broadening of residues that undergo large chemical shift changes in either the nonspecific, noncognate, or cognate complexes. This argues that if the protein is transiently flipping out bases in noncognate or nonspecific complexes, this process is either fast enough to minimize exchange broadening or so slow that the residues of the minority flipped out forms are too weak to be observed as distinct resonances.

ACKNOWLEDGMENT

The authors thank Whitney Shatz for preparation of the $^{2}H/^{15}N/^{13}C$-labeled protein for the unmethylated cognate DNA complex.

SUPPORTING INFORMATION AVAILABLE

Three figures showing $^{1}H-^{15}N$ TROSY-HSQC spectra, one with assignments for the M.HhaI−AdoHcy−hemimethylated cognate DNA complex, one showing differences between M. HhaI bound with hemimethylated cognate and unmethylated cognate DNA, and one showing differences between M.HhaI bound with nonspecific and noncognate DNA. This material is available free of charge via the Internet at http://pubs.acs.org.

REFERENCES

1. Jeltsch, A. (2002) Beyond Watson and Crick: DNA methylation and molecular enzymology of DNA methyltransferases. *ChemBioChem 3*, 274–293.
2. Jeltsch, A. (2002) Erratum: Beyond Watson and Crick: DNA methylation and molecular enzymology of DNA methyltransferases. *ChemBioChem 3*, 382.
3. Mai, A., and Altucci, L. (2009) Epi-drugs to fight cancer: from chemistry to cancer treatment, the road ahead. *Int. J. Biochem. Cell Biol. 41*, 199–213.
4. Mashhoon, N., Pruss, C., Carroll, M., Johnson, P. H., and Reich, N. O. (2006) Selective inhibitors of bacterial DNA adenine methyltransferases. *J. Biomol. Screening 11*, 497–510.
5. Naumann, T. A., Tavassoli, A., and Benkovic, S. J. (2008) Genetic selection of cyclic peptide Dam methyltransferase inhibitors. *ChemBioChem 9*, 194–197.
6. Viadiu, H., and Aggarwal, A. K. (2000) Structure of BamHI bound to nonspecific DNA: a model for DNA sliding. *Mol. Cell 5*, 889–895.
7. Banerjee, A., Santos, W. L., and Verdine, G. L. (2006) Structure of a DNA glycosylase searching for lesions. *Science 311*, 1153–1157.
8. Winkler, F. K., Banner, D. W., Oefner, C., Tsernoglou, D., Brown, R. S., Heathman, S. P., Bryan, R. K., Martin, P. D., Petratos, K., and Wilson, K. S. (1993) The crystal structure of EcoRV endonuclease and of its complexes with cognate and non-cognate DNA fragments. *EMBO J. 12*, 1781–1795.
9. Kalodimos, C. G., Biris, N., Bonvin, A. M. J. J., Levandoski, M. M., Guennuegues, M., Boelens, R., and Kaptein, R. (2004) Structure and flexibility adaptation in nonspecific and specific protein-DNA complexes. *Science 305*, 386–389.
10. Iwahara, J., and Clore, G. M. (2006) Detecting transient intermediates in macromolecular binding by paramagnetic NMR. *Nature 440*, 1227–1230.
11. Iwahara, J., Zweckstetter, M., and Clore, G. M. (2006) NMR structural and kinetic characterization of a homeodomain diffusing and hopping on nonspecific DNA. *Proc. Natl. Acad. Sci. U.S.A. 103*, 15062–15067.
12. Dupureur, C. M. (2005) NMR studies of restriction enzyme-DNA interactions: role of conformation in sequence specificity. *Biochemistry 44*, 5065–5074.
13. Lukasik, S. M., Cierpicki, T., Borloz, M., Grembecka, J., Everett, A., and Bushweller, J. H. (2006) High resolution structure of the HDGF PWWP domain: a potential DNA binding domain. *Protein Sci. 15*, 314–323.
14. Bonnet, I., Biebricher, A., Porté, P., Loverdo, C., Bénichou, O., Voituriez, R., Escudé, C., Wende, W., Pingoud, A., and Desbiolles, P. (2008) Sliding and jumping of single EcoRV restriction enzymes on non-cognate DNA. *Nucleic Acids Res. 36*, 4118–4127.
15. Peterson, S. N., Dahlquist, F. W., and Reich, N. O. (2007) The role of high affinity non-specific DNA binding by Lrp in transcriptional regulation and DNA organization. *J. Mol. Biol. 369*, 1307–1317.
16. Sidorova, N. Y., and Rau, D. C. (1996) Differences in water release for the binding of EcoRI to specific and nonspecific DNA sequences. *Proc. Natl. Acad. Sci. U.S.A. 93*, 12272–12277.
17. Sidorova, N. Y., Muradymov, S., and Rau, D. C. (2006) Differences in hydration coupled to specific and nonspecific competitive binding and to specific DNA binding of the restriction endonuclease BamHI. *J. Biol. Chem. 281*, 35656–35666.
18. Kao-Huang, Y., Revzin, A., Butler, A. P., O'Conner, P., Noble, D. W., and von Hippel, P. H. (1977) Nonspecific DNA binding of genome-regulating proteins as a biological control mechanism: measurement of DNA-bound *Escherichia coli* lac repressor in vivo. *Proc. Natl. Acad. Sci. U.S.A. 74*, 4228–4232.
19. Cheng, X., Kumar, S., Posfai, J., Pflugrath, J. W., and Roberts, R. J. (1993) Crystal structure of the HhaI DNA methyltransferase complexed with S-adenosyl-L-methionine. *Cell 74*, 299–307.
20. Klimasauskas, S., Kumar, S., Roberts, R. J., and Cheng, X. (1994) HhaI methyltransferase flips its target base out of the DNA helix. *Cell 76*, 357–369.
21. O'Gara, M., Klimasauskas, S., Roberts, R. J., and Cheng, X. (1996) Enzymatic C5-cytosine methylation of DNA: mechanistic implications of new crystal structures for HhaI methyltransferase-DNA-AdoHcy complexes. *J. Mol. Biol. 261*, 634–645.
22. O'Gara, M., Roberts, R. J., and Cheng, X. (1996) A structural basis for the preferential binding of hemimethylated DNA by HhaI DNA methyltransferase. *J. Mol. Biol. 263*, 597–606.
23. O'Gara, M., Zhang, X., Roberts, R. J., and Cheng, X. (1999) Structure of a binary complex of HhaI methyltransferase with S-adenosyl-L-methionine formed in the presence of a short non-specific DNA oligonucleotide. *J. Mol. Biol. 287*, 201–209.
24. Estabrook, R. A., and Reich, N. (2006) Observing an induced-fit mechanism during sequence-specific DNA methylation. *J. Biol. Chem. 281*, 37205–37214.

25. Lindstrom, W. M., Flynn, J., and Reich, N. O. (2000) Reconciling structure and function in HhaI DNA cytosine-C-5 methyltransferase. *J. Biol. Chem. 275*, 4912–4919.
26. Youngblood, B., Buller, F., and Reich, N. O. (2006) Determinants of sequence-specific DNA methylation: target recognition and catalysis are coupled in M.HhaI. *Biochemistry 45*, 15563–15572.
27. Zhou, H., Shatz, W., Purdy, M. M., Fera, N., Dahlquist, F. W., and Reich, N. O. (2007) Long-range structural and dynamical changes induced by cofactor binding in DNA methyltransferase M.HhaI. *Biochemistry 46*, 7261–7268.
28. Daujotyte, D., Vilkaitis, G., Manelyte, L., Skalicky, J., Szyperski, T., and Klimasauskas, S. (2003) Solubility engineering of the HhaI methyltransferase. *Protein Eng. 16*, 295–301.
29. Gardner, K. H., and Kay, L. E. (1998) The use of ^{2}H, ^{13}C, ^{15}N multidimensional NMR to study the structure and dynamics of proteins. *Annu. Rev. Biophys. Biomol. Struct. 27*, 357–406.
30. Pervushin, K., Riek, R., Wider, G., and Wuthrich, K. (1997) Attenuated T2 relaxation by mutual cancellation of dipole-dipole coupling and chemical shift anisotropy indicates an avenue to NMR structures of very large biological macromolecules in solution. *Proc. Natl. Acad. Sci. U.S.A. 94*, 12366–12371.
31. Yang, D., and Kay, L. (1999) Improved lineshape and sensitivity in the HNCO-family of triple resonance experiments. *J. Biomol. NMR 14*, 273–276.
32. Rance, M., Loria, J. P., and Palmer, A. G.III (1999) Sensitivity improvement of transverse relaxation-optimized spectroscopy. *J. Magn. Reson. 136*, 92–101.
33. Salzmann, M., Pervushin, K., Wider, G., Senn, H., and Wuthrich, K. (1998) TROSY in triple-resonance experiments: new perspectives for sequential NMR assignment of large proteins. *Proc. Natl. Acad. Sci. U.S.A. 95*, 13585–13590.
34. Yamazaki, T., Lee, W., Arrowsmith, C. H., Muhandiram, D. R., and Kay, L. E. (1994) A suite of triple resonance NMR experiments for the backbone assignment of ^{15}N, ^{13}C, ^{2}H labeled proteins with high sensitivity. *J. Am. Chem. Soc. 116*, 11655–11666.
35. Kay, L. E., Ikura, M., Tschudin, R., and Bax, A. (1990) Three dimensional triple-resonance NMR spectroscopy of isotopically enriched proteins. *J. Magn. Reson. 89*, 496–514.
36. Youngblood, B., Shieh, F., De Los Rios, S., Perona, J. J., and Reich, N. O. (2006) Engineered extrahelical base destabilization enhances sequence discrimination of DNA methyltransferase M.HhaI. *J. Mol. Biol. 362*, 334–346.
37. Wishart, D. S., and Sykes, B. D. (1994) The ^{13}C chemical-shift index: a simple method for the identification of protein secondary structure using ^{13}C chemical-shift data. *J. Biomol. NMR 4*, 171–80.
38. Spera, S., and Bax, A. (1991) Empirical correlation between protein backbone conformation and Cα and Cβ ^{13}C nuclear magnetic resonance chemical shifts. *J. Am. Chem. Soc. 113*, 5490–5492.
39. Dubey, A. K., and Roberts, R. J. (1992) Sequence-specific DNA binding by the MspI DNA methyltransferase. *Nucleic Acids Res. 20*, 3167–3173.
40. Szczelkun, M. D., and Connolly, B. A. (1995) Sequence-specific binding of DNA by the EcoRV restriction and modification enzymes with nucleic acid and cofactor analogues. *Biochemistry 34*, 10724–10733.
41. Bahadur, R. P., Zacharias, M., and Janin, J. (2008) Dissecting protein-RNA recognition sites. *Nucleic Acids Res. 36*, 2705–2716.
42. Nadassy, K., Wodak, S. J., and Janin, J. (1999) Structural features of protein-nucleic acid recognition sites. *Biochemistry 38*, 1999–2017.
43. Schreiber, G. (2002) Kinetic studies of protein-protein interactions. *Curr. Opin. Struct. Biol. 12*, 41–47.
44. Sheinerman, F. B., Norel, R., and Honig, B. (2000) Electrostatic aspects of protein-protein interactions. *Curr. Opin. Struct. Biol. 10*, 153–159.
45. Hemsath, L., Dvorsky, R., Fiegen, D., Carlier, M., and Ahmadian, M. R. (2005) An electrostatic steering mechanism of Cdc42 recognition by Wiskott-Aldrich syndrome proteins. *Mol. Cell 20*, 313–324.
46. Kiel, C., Selzer, T., Shaul, Y., Schreiber, G., and Herrmann, C. (2004) Electrostatically optimized Ras-binding Ral guanine dissociation stimulator mutants increase the rate of association by stabilizing the encounter complex. *Proc. Natl. Acad. Sci. U.S.A. 101*, 9223–9228.
47. Banavali, N. K., and MacKerell, A. D. (2002) Free energy and structural pathways of base flipping in a DNA GCGC containing sequence. *J. Mol. Biol. 319*, 141–60.
48. Giudice, E., Várnai, P., and Lavery, R. (2003) Base pair opening within B-DNA: free energy pathways for GC and AT pairs from umbrella sampling simulations. *Nucleic Acids Res. 31*, 1434–1443.
49. Gueron, M., and Leroy, J. L. (1992) Base-pair opening in double-stranded nucleic acids. In *Nucleic Acids and Molecular Biology* (Eckstein, F., and Lilley, D. M. J., Eds.) pp 1−22, Vol. 6, Springer-Verlag, New York.
50. Jeltsch, A., Alves, J., Wolfes, H., Maass, G., and Pingoud, A. (1994) Pausing of the restriction endonuclease EcoRI during linear diffusion on DNA. *Biochemistry 33*, 10215–10219.
51. Townson, S. A., Samuelson, J. C., Bao, Y., Xu, S., and Aggarwal, A. K. (2007) BstYI bound to noncognate DNA reveals a "hemispecific" complex: implications for DNA scanning. *Structure 15*, 449–459.
52. Shieh, F., Youngblood, B., and Reich, N. O. (2006) The role of Arg165 towards base flipping, base stabilization and catalysis in M. HhaI. *J. Mol. Biol. 362*, 516–527.